final report

Project code: L.BSC.0001

Prepared by: Alen Alempijevic
University of Technology Sydney

Date published: 08 August 2017

PUBLISHED BY
Meat and Livestock Australia Limited
Locked Bag 1961
NORTH SYDNEY NSW 2059

3D imaging for phenotypic trait estimation of beef and sheep carcasses

Meat & Livestock Australia acknowledges the matching funds provided by the Australian Government to support the research and development detailed in this publication.

Executive summary

The project builds upon initial proof of concept work reported under "Value based trading system: image analysis of sheep and beef carcasses- proof of concept" (MLA project no: B.SBP.0121) where the technique for estimation of objective traits was undertaken based on 3D shape curvature descriptors.

Developing a prototype scanning rig capable of capturing data with high fidelity 3D images in abbatoir settings was a crucial objective for this project. An approach to 3D carcass construction was developed using the rotating rig with three 3D cameras via a batch optimisation framework (g2o) to compute the best fit of all data into a common representation of the carcass. A sensor fusion pipeline with dense 3D information giving more coverage over the carcass and increased robustness to sensor noise was designed. This work has further allowed an evaluation of possibilities for speeding up the up the acquisition process of the 3D scanner. The system was tested for a total of 15 days in non-sray chillers at 3 commercial abbatoirs (beef and lamb).

Alterations to the fusion method for assembling 3D models of the carcass have been undertaken to allow more robustness in the estimation framework. The curvatures of the hindquarter produced a strong relationship between lean mean yield [%] of beef carcasses on a combined dataset (n=69) acquired over 3 slaughters with a 4.05 root mean square error (RMSE) and 0.7 R^2 in estimating lean meat yield (LMY).

Porting of the 3D curvature approach for estimating LMY on beef carcasses could not be applied to lamb carcasses. Beef carcasses are halved in the abattoir chain, thus, the internal surface of musculoskeletal composition of the carcass is exposed. In contrast to the internal surfaces of the beef carcass, lamb carcasses have smooth curvatures and no correspondence of curvature to LMY was established. An alternative proposition to estimate subcutaneous fat cover using Hyperspectral Imaging has been preliminarly evaluated for improving accuracy of LMY estimation. Hyperspectral Image data was transformed to use reflectance as the feature that is invariant to the respective position of camera and light source. In a laboratory setting on a dataset of 16 lamb cuts the approach produced 0.92 R^2 and 0.8mm root mean square error (RMSE) in estimating fat depths up to 12mm.

Precise delineation of muscle groups from 3D data is proposed as an important refinement to imrpove the accuracy of 3D imaging. Methods for determining carcass fat, combining Hyperspectral and 3D data on the sensing rig are recommended as future work with a view to evaluating the system on whole carcasses.

Table of contents

1 Background

This project builds upon our previous work under "Value based trading system: image analysis of sheep and beef carcasses- proof of concept" (MLA project no: B.SBP.0121) which investigated application of 3D imaging on trait estimation of carcasses. Given 3D imaging solely captures the outside surface of carcass, the technique investigated does not have the potential to produce trait prediction at the accuracy of penetrating technology (medical CT). Rather, the technology is evaluated for accuracy given significantly reduced cost; RGBD sensors used to produce 3D imaging are now a commodity hardware.

In B.SBP.0121, acquiring 3D beef carcass data using a handheld scanning device was undertaken and a relationship between curvature of the hindquarter region of the beef carcass and lean meat yield (LMY) quantified. An early prototype rig was developed to accomplish automatic capturing of 3D data and tested on a single lamb carcass in a laboratory setting (UNE chillers), validating the potential of an automated data collection method. Work on devising a rig that could be part of abattoir processing chain was warranted and to be undertaken as part of extension work.

Muscle groups compromising the hindquarter, used to develop the relationship between curvature and trait, when used with 3D imaging are ascertained from the external surface. In the abattoir a beef carcass is halved and suspended on the processing chain, the internal structure of the beef carcass is exposed and elements of the musculoskeletal composition of the carcass are visible. Conversely, access to the internal rib bone structure of the lamb carcass is not possible while scanning for 3D images. Therefore, apart from the techniques developed for trait estimation from 3D Imaging data in B.SBP.0121 study on beef carcasses, deemed applicable to the sheep carcasses, extraction of surface and volume was also investigated.

During the project, a number of activities aligned with the Department of Agriculture and Water Resources Rural R&D for Profit funded *Advanced Livestock Measurement Technologies* project (ALMTech - MLA project no: V.RDP.2005) which commenced in 2016. The opportunity to evaluate devices reporting Lean Meat Yield against a gold standard CT calibrated data set were presented, rather than performing commercial bone-outs as proposed on the onset of the project. Therefore, evaluation of the methodology based on machine learning prediction techniques and continuous improvements of scanning process were pursued.

Finally, the opportunity to use Hyperspectral imagery was explored to complete objectives of the project of estimating LMY in lamb carcasses. Though 3D curvatures are not immensely pronounced on the lamb carcass, lambs visibly deposit subcutaneous fat (fat cover). Hyperspectral imagery has potential to discriminate muscle and fat and is being developed to estimate meat quality. Therefore, extending the capabilities to determine fat depth was evaluated on lamb cuts. Combining Hyperspectral data with 3D data to create a fat cover profile is considered as an opportunity to leverage both technologies in a novel way and allow for total fat estimation beyond the single point GR measurement.

2 Project objectives

The objectives specified for the project are:

- Determine the best camera position for estimating Lean Meat Yield in lamb carcasses,
- Develop and validate the machine learning of 3D images of lamb carcasses to estimate lean meat yield,
- Benchmark prediction accuracy in commercial processing conditions against CT (lamb) and CT or commercial bone out (beef),
- Deliver prototype devices to estimate traits of carcass.

To complete stated objectives the project aimed to:

- Evaluate suitable camera motion to capture 3D images of carcase within abattoir operational constraints and consequently undertake modifications to scanning equipment to increase the speed of taking 3D images.
- Develop application of the technology to capture and reconstruct 3D images without significantly interrupting motion of the processing chain for beef/sheep abattoirs.
- Develop estimation of CT lean meat yield in lamb carcasses.
- Capture 3D images of lamb carcasses in an abattoir that has a DEXA system installed.
- Compare CT lean meat yield between 3D camera technology and the DEXA system.
- Take 3D images of beef carcasses in an abattoir and perform a commercial bone out to determine the accuracy of estimating RBY specific to that abattoir.
- Improve the efficiency of 3D representation and improve the machine learning capabilities.
- Incorporate live weight or hot carcass weight (HCW) into the estimation system of carcasses.
- Evaluate the data and report on the accuracy of estimation

3 Methodology

3.1 Carcass Data

Beef and lamb carcasses were acquired over the duration of the project, with the assistance of JBS Bordertown, JBS Brooklyn and TEYS Wagga Wagga.

3.1.1 Beef Carcass Data

Three data collections form part of the work reported. Serial slaughters at John Dee Warwick (May 2014), TEYS Wagga Wagga (30 May – 2 June 2016) and JBS Brooklyn (10 – 21 October 2016).

The carcasses scanned as part of B.BSP.0121 (Serial Kill 4 at John Dee Warwick) contained 30 carcasses, for which both 3D handheld scanning and CT scanning has taken place. Cattle in this dataset were 97 days on feed. TEYS serial slaughter were part of a BeefSpecs evaluation study on steers after 134 days of feed. The carcasses at JBS Brooklyn were part of a study evaluating the DEXA system and embodied a range of traits of cattle (carcasses consisted of cows, steers and heifers).

After slaughter carcasses were moved into non spray chillers and 3D images of the carcasses were taken. At TEYS Wagga Wagga 3D data of hot carcasses was obtained while at JBS Brooklyn 3D data of carcasses were acquired approximately 20 hours post mortem. This resulted in the acquisition of 30, 28 and 47 carcasses respectively with the 3D scanning rig.

The Computed Tomography (CT) scanned data from B.BSP.0121 (Serial Kill 4) contains the division of cold carcass weight (CCWT) into lean, fat and bone weight, thus containing the LMY. The same approach was undertaken for JBS Brooklyn data. The results of LMY where produced by NSW DPI and Murdoch University respectively. The LMY data from TEYS Wagg Wagga kills was derived from the chuck and rump primals of the 28 carcases by NSW DPI. CT images were taken of the 2 primals (chuck and rump) and the amount of lean muscle and fat (intramuscular, subcutaneous and intermuscular fat depots) in the primals was determined (reported in MS4).

Combined data resulted in a wide range of live weights, carcass weight and Lean Meat Yield values. The distribution of Lean Meat Yield % (for the carcass side) over the entire dataset is denoted in Fig. 1. The JBS Brooklyn data covers a wider range of animals, and less resembles the animals slaughtered through the chains of TEYS Wagga Wagga and John Dee Warwick, where carcasses were from 97 and 134 days on feed.

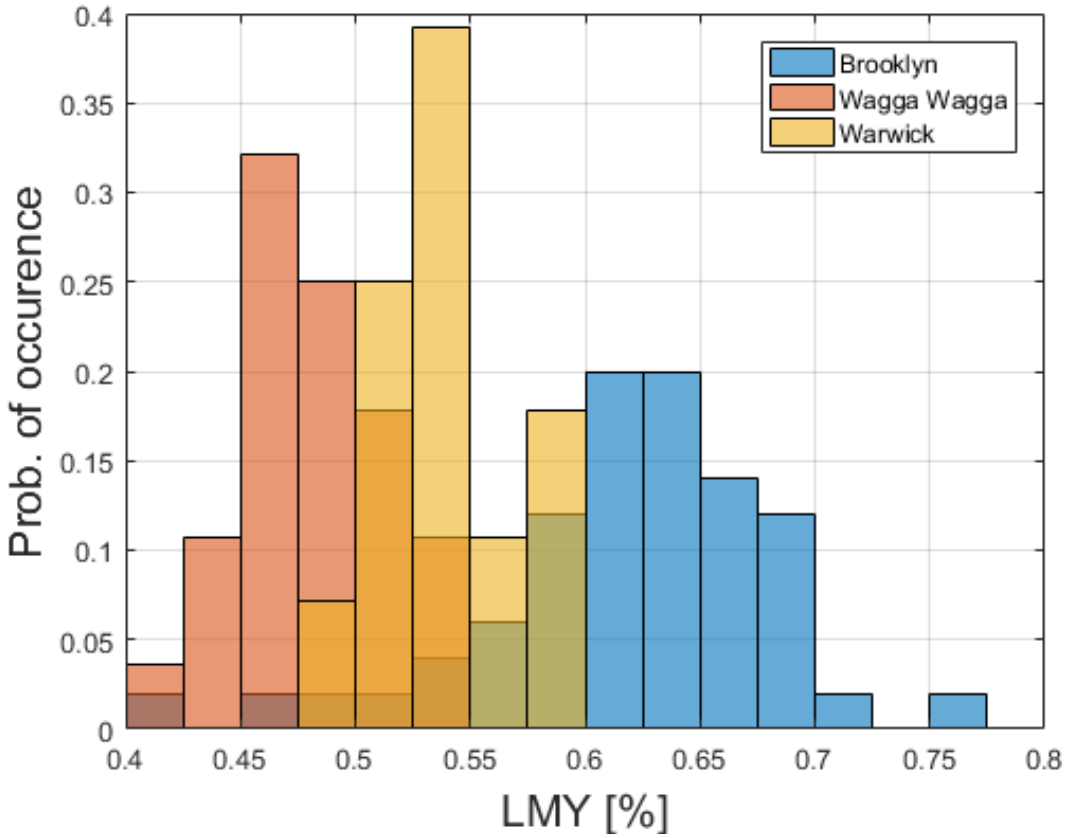

Fig. 1 – The Probability Density Function of Lean [%] of the three combined datasets. John Dee Warwick (yellow), TEYS Wagga Wagga (red) and JBS Brooklyn (blue)

Table 1 – Data collected over project lifespan and data used

Kill Date	Carcass Data Statistics				Location
	Available	3D Scanned	3D Processed	Whole CT	
May 2014	31	30	29	YES	John Dee - Warwick
May 2016	28	28	15	NO	TEYS – Wagga Wagga
Oct 2016	51	47	25	YES	JBS - Brooklyn
TOTAL	**110**	**105**	**69**		

3.1.2 Lamb Carcass Data

Data collection were undertaken at four serial slaughters at JBS Bordertown (period July – September 2015). After slaughter carcasses moved along the chain and were fully processed. The carcasses then moved into chillers and 3D images of the carcasses were taken resulting in a total of n=281 scanned carcasses from the available 400 carcasses as per Table 2. The carcasses scanned in each serial slaughter were selected to embody a range of traits. Overall, carcass selection was coordinated by SARDI and Murdoch University.

The CT scanned data from each slaughter, referred to as the 'gold standard' measure of carcass composition, contains the division of cold carcass weight (CCWT) into lean, fat and bone weight. Data from all serial slaughters wwere provided to enable analysis in this report.

Table 2 - 3D Scanning Tool participation in JBS Bordertown Trials

Serial Kill Date	Kill #	Available Carcasses	Scanned Carcasses	Scanning Technique
July 2015	2	100	74	Handheld
August 2015	4	100	62	Handheld
September 2015	5	100	62	Handheld
September 2015	6	100	83	Scanner Rig
TOTAL		**400**	**281**	

3.2 Capturing 3D Carcass Data

Early beef carcass data captured at John Dee (B.SBP.0121), as well as lamb carcass data collection in initial three kills within this project, was completed *via* a hand held RGBD camera (Primesense 1.09). Hypotheses over the optimal method of moving the sensor with respect to coverage of the carcass and completeness of the 3D model were evaluated. Insights gained were incorporated into development and deployment of the carcass scanning rig, initially deployed in Kill #6 at JBS Bordertown Fig. 2 (left). The scanning rig was designed to be ammendable for use on beef carcasses and validated in subsequent deployments.

3D data collection was achieved using a carcass scanning rig designed for either lamb or beef carcasses. The rig is configurable, and has been extended to accommodate beef carcasses. The first deployment of the Beef Scanning Rig was in May 2016 at TEYS Wagga Wagga.

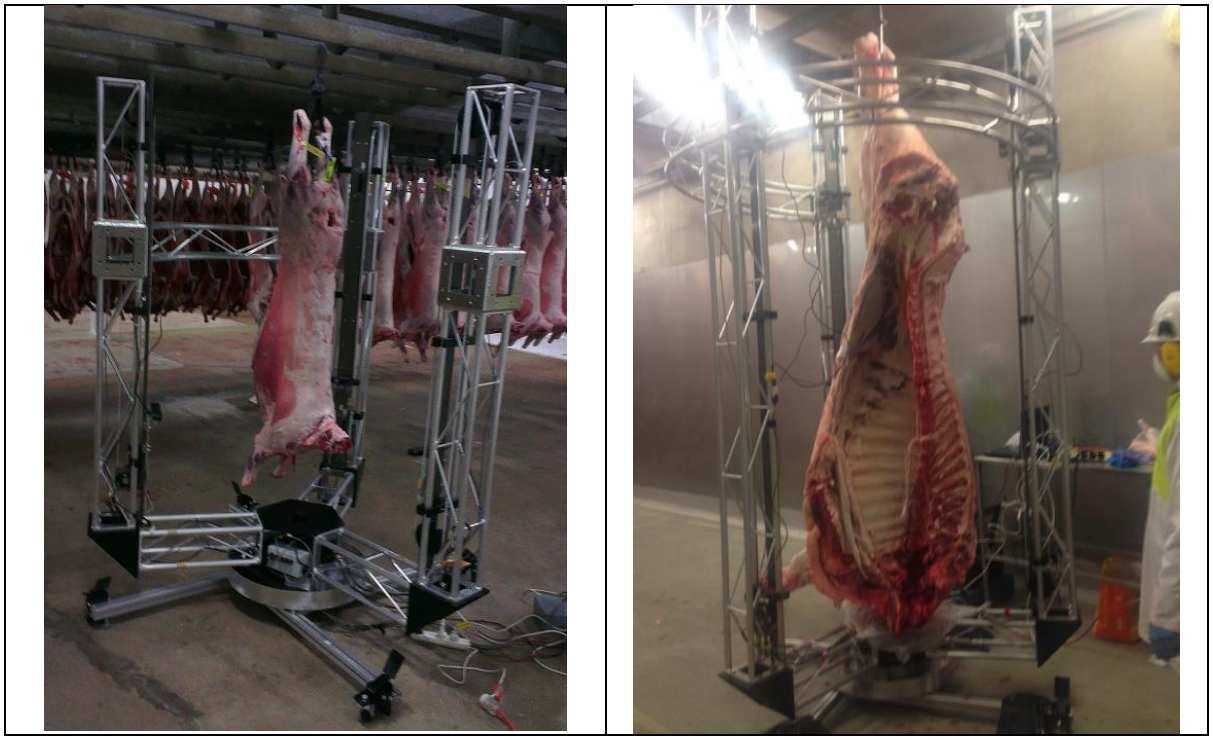

Fig. 2 – Scanning Rig evaluated at: (right) JBS Bordertown 30 September 2015, and (left) TEYS Wagga Wagga 30 May – 2 June 2016

The sequence of images from the cameras (referred to as frames) is acquired as the cameras move up/down and as the rig rotates. Each camera on the rig is offset by 120° from the other cameras. This is a design requirement enforced by the structured light imaging technique employed as a single depth projection source can solely illuminate a part of the carcass (Zanuttigh, 2016). Therefore, with the structured light 3D camera sensing technology produced up to 2016 (Zanuttigh, 2016), it is not possible to have more cameras on the rig due to interference, overlapping cameras will not provide any data in regions with overlap.

The rig design mediates issues in interference in cameras and enables capturing the entire carcass due to two design elements: rotation of the base and up/down camera motion. Due to travel up/down and rotation of 120° each camera in the scanning process observes 180° of the carcass. The rig rotation also creates a 60° overlap between areas exposed to the cameras which assists in fusing the different camera views together.

The displacement between the vertical elements of the camera rig enables an effective clearance.

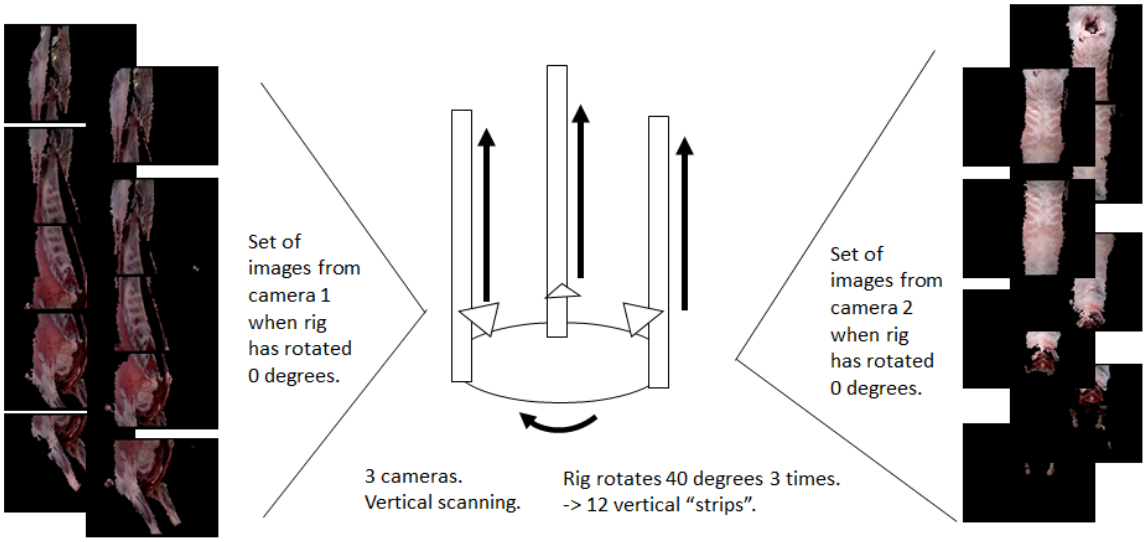

Fig. 3 – Scanning Process

Two different methods were used for storing sequences of camera data. For some carcasses, the camera data was stored as a single sequence of images per camera, per carcass. For other carcasses, camera data was stored in separate sequences each time the camera changed directions (up/down).

3.2.1 3D Data Processing

A two-phase approach presented in Fig. 3 was used to build a 3D model from the images taken by the multiple cameras on the scanning rig, particularly in the case where the carcass is swinging.

In this project, as part of devising a scanning rig, mediating the rotation and sway of the carcass body around the pivotal axis is handled. The sheep carcasses in the chillers did not exhibit rotation as those of beef carcasses. General weight and moment of inertia of a beef carcass are vastly larger and more susceptible to motion. Nevertheless, the problem was investigated by arbitrary swinging the carcass as it were on a production chain and being abruptly stopped. The approach requires simultaneous estimation of the position of cameras during scanning, and that of the carcass as a pendulum in motion denoted in Fig. 4. The camera motion relative to the carcass (when the carcass is selected as the stationary object) is depicted in Fig. 5.

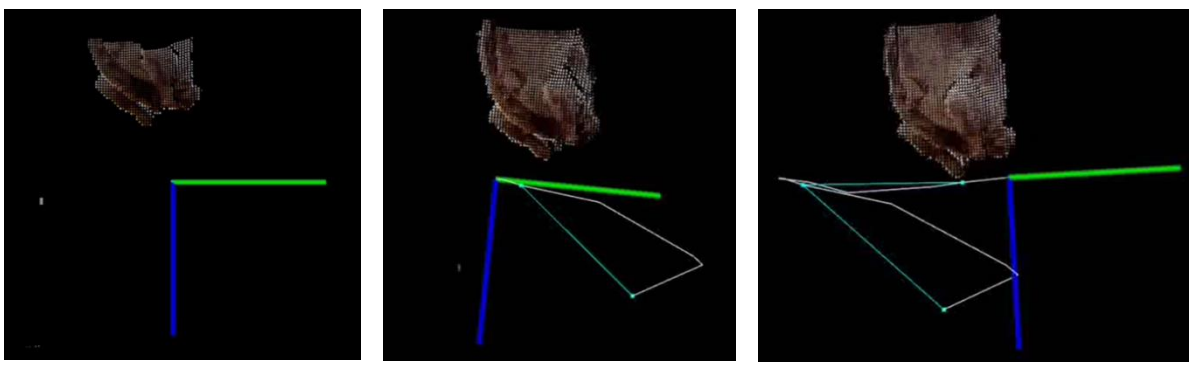

Fig. 4 - Simultaneously estimating position of camera and pose of carcass during swinging

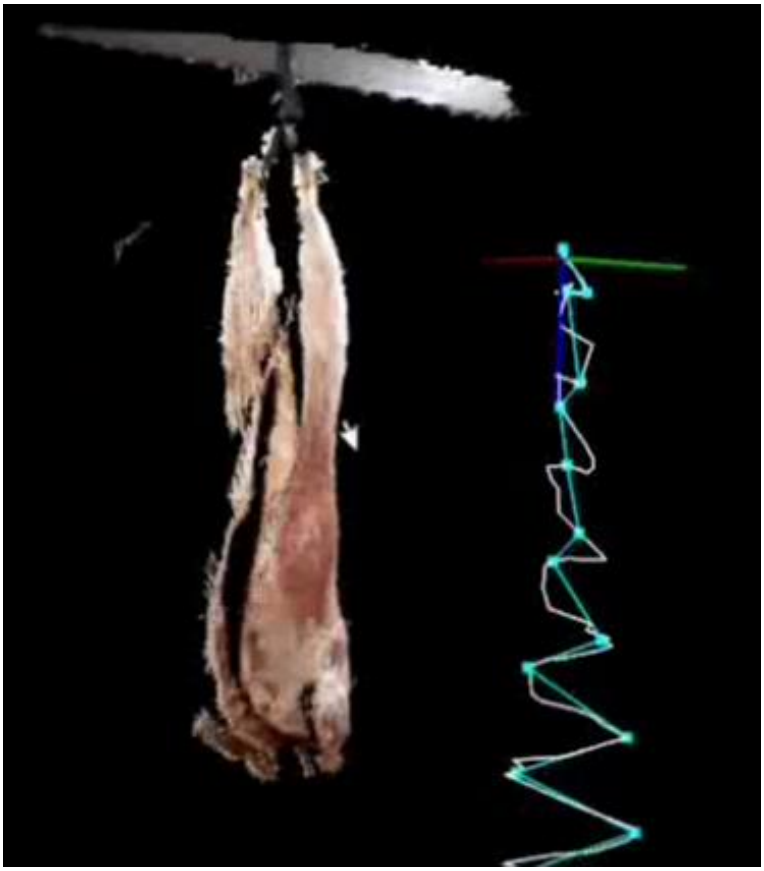

Fig. 5 - 3D model of one side of carcass (left) and the complete carcass motion during swinging depicted (right)

Fusing the images into a single 3D model takes place in four steps, as per Fig. 6, which has aided automation, and resulted in a streamlined processing framework with more reliable output, and resilience to any missing data (motion blur when swinging of carcass).

The frames from each camera are compared to that of neighbouring cameras and are now jointly used to determine commonalities between frames. The raw colour camera images are used in combination with 3D data to find correspondences between frames. Matching of 2D points and 3D locations is used to create a dense graph of the possible trajectories and 3D points, as denoted in Fig. 6. Each node in the graph is a camera frame (in computer vision community this is referred to as a camera pose in 6DOF) during the trajectory taken to capture the entire carcass.

This graph is fed into a state of the art framework for optimizing graph-based nonlinear error functions, noted as g2o (Kuemmerle, 2011). The framework deals with outliers, noise, and produces the optimised trajectory of the series of cameras frames (noted as nodes of the graph) and vertices (connections between cameras frames).

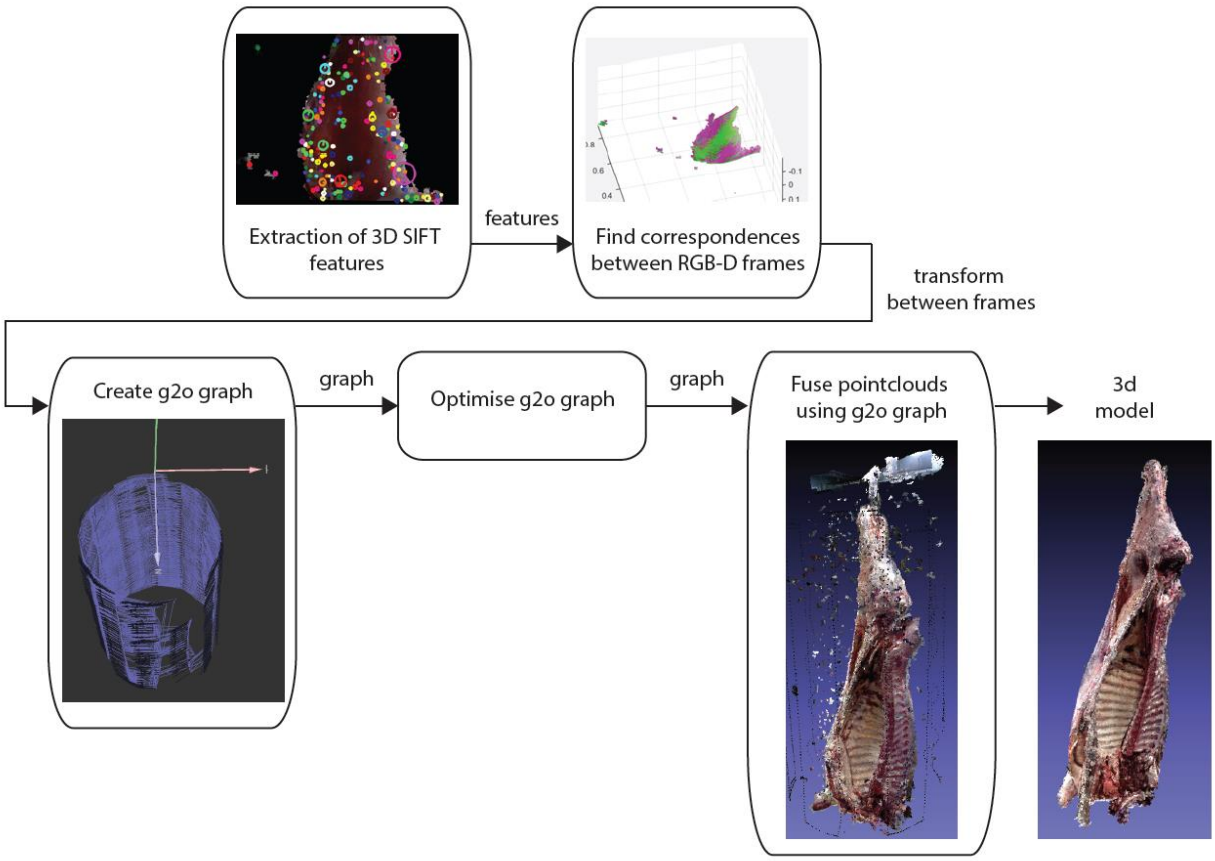

Fig. 6 – Steps of generating 3D model from top left in order of connected components of the graph. (1) Obtaining visual features, (2) finding correspondences between two images (3) creating a graph representation of camera frames and optimising it to obtain the trajectory of all cameras, (5) fusing 3D points from individual frames into a single 3D model and (5) 3D model after removal of spurious points

The process of matching frames attempts to match at varying densities, at various windows of interest (e.g. a frame is matched to each of the next five frames, then every fifth frame after that for the next five matches, then every tenth frame after that for the next five matches). This new pattern of matching allows for very robust sequential stitching of data from a single camera, particularly the longer camera sequences, and even allows for recovery of large camera rotation information. The results on the data from an example carcass can be seen in Fig. 7. Note that despite the poor prior camera poses provided, the density of matches found is sufficient to recover camera trajectory.

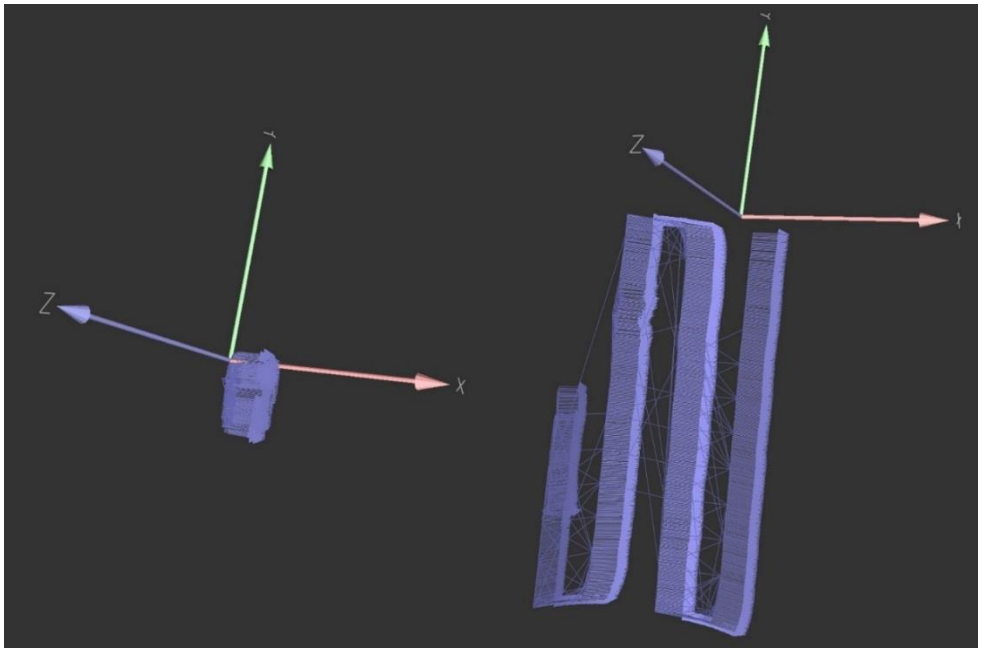

Fig. 7 – Camera sequence before (left) and after optimisation (right)

A further processing step has also been added to the pipeline for removing outlier frames (3D point clouds from current camera view that cannot be combined into the whole carcass 3D representation). Outlier frames occur when poor quality matches result in a frame being placed in a position very different from the preceding and following frames. This problem typically occurs in scenarios where depth or RGB data is missing from part of a camera's trajectory. During scanning of carcasses this problem has been encountered with the >600kg live weight carcasses. Due to the floor space constraints at John Dee and TEYS (in order to limit occupying a single chain in chiller), the radius of the scanner is restricted to 600mm. However, the carcasses with large size (grain finished) encroached the sensing limits of the cameras (30cm) and have resulted in limited depth information.

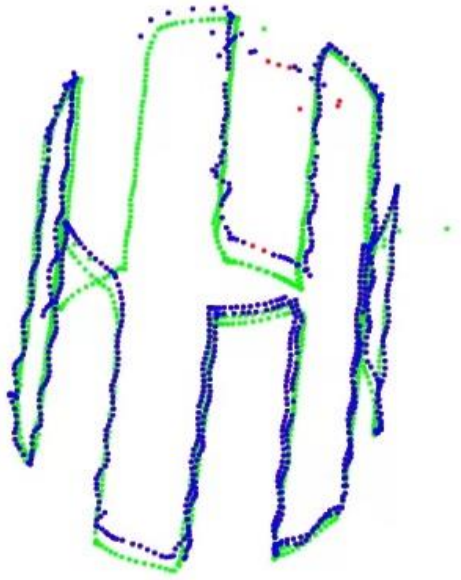

Fig. 8 – Outlier removal using prior example. Shown in green is a prior trajectory from a well-fused carcass. In blue the camera trajectories for the carcass currently being fused, and in red the frames considered outliers based on distance from the prior.

As shown in Fig. 8, outlier frames in the camera trajectory currently being fused can be discovered based on their distance from a prior model. The model is based on a previously fused cameras trajectory for a different carcass. Once the camera frames have been optimised, a fused colour pointcloud of all the camera images can be generated, as shown in Fig. 6. A Poisson surface is fitted to this pointcloud to remove noise from the sensor data. The Poisson surface is then segmented and turned into a set of points representing the curvature of the region of interest of the carcass, shown in Fig. 9

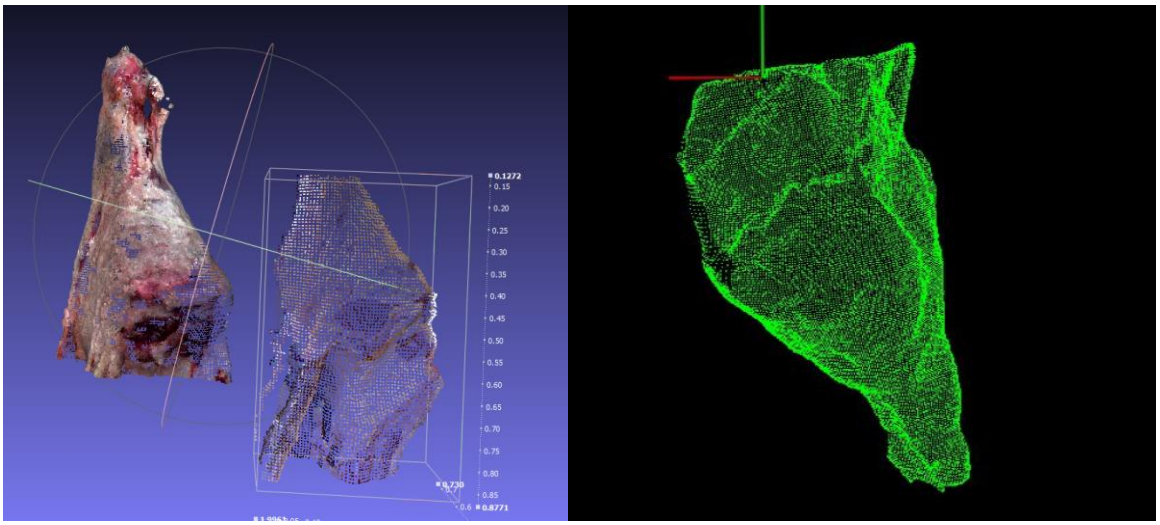

Fig. 9 - Complete area of the hindquarter is scanned (left) Hindquarter regions left with colour (right) hindquarter without colour and axis aligned for processing. The new pipeline produces much denser data, evident in comparison of data from Sep 2013 and May 2016.

3.3 Lamb Cuts - Specimen Data

3.3.1 Capturing Hyperspectral Camera Data

For the purposes of evaluating this approach, an experimental setup in a laboratory setting was devised. Specimens, cuts of lamb from loin and rump regions, were placed on a surface allowing them to be simultaneously seen by a RGB camera and a Hyperspectral camera (Resonon Pika NR) shown in Figure 10. The hyperspectral camera captures lines of data, thus the specimen was moved vertically to generate a full side profile of the cut, as presented in Figure 10. The RGB camera was used to obtain the "ground truth" of the actual fat depth, achieved by semi-automated labelling of the cut.

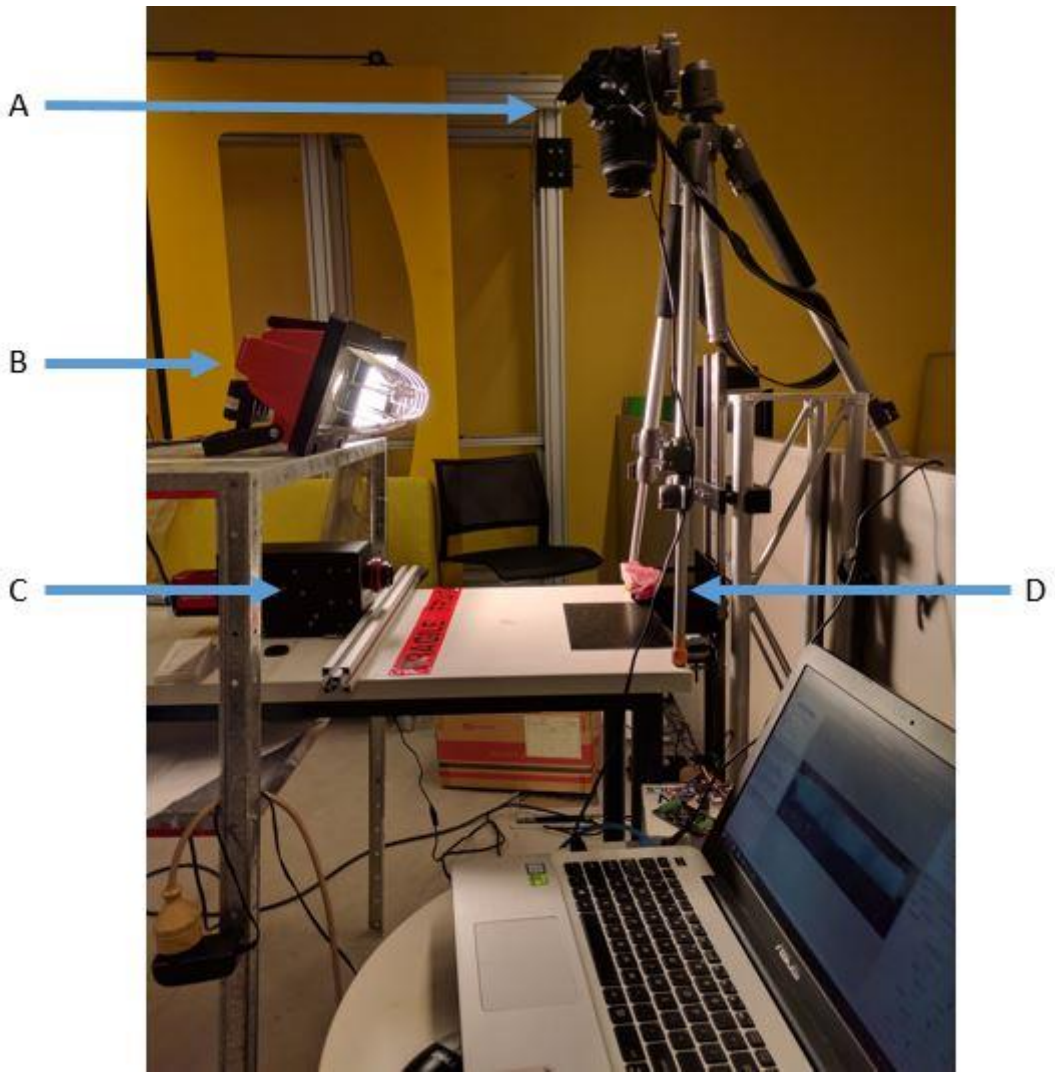

Fig. 10 - Gathering data for Fat Estimation on current laboratory setup. (A) RGB camera to obtain the "ground truth" of the actual fat depth, by examining the cut top-down, (B) Light source to illuminate scene, (C) Hyperspectral camera which is looking

3.3.2 Hyperspectral Data Processing

As curvatures are not sufficiently pronounced on the lamb carcass as the carcass is not cut into sides, the use of the Hyperspectral imagery is being explored to discriminate muscle and fat, and extending the capabilities of the system to determine fat depth. The identification of fat and non-fat pixels is

posed as a classification problem where object reflectance, instead of image intensity or radiance, is used as the feature for classification. Reflectance, being a unique photometric property of an object, provides discriminative information about the object and is invariant to changes in illumination directions, illumination power spectra and object shapes.

Reflectance, unlike radiance, cannot be directly obtained from an image. Since object shape, reflectance, and illumination coexist and collectively compose an image of a scene, recovery of reflectance also requires the separation and recovery of these geometric and photometric factors. From a computational perspective, estimating the photometric and geometric properties from a single input image is an under-constrained problem. To render the problem well posed, the information-rich representation of Hyperspectral Imaging is used to deliver wavelength-indexed data in hundreds of bands across the NIR spectrum. In addition, as reflectance is a wavelength-dependent property, it also demands the use of spectral images in the parameter estimation problem.

Following the state-of-the-art approaches based on Hyperspectral Imaging (Huynh and Robles-Kelly 2010, Rahman 2013), the problem of recovering reflectance is addressed through an estimation of the illumination power spectrum, the shading and specularity from a single Hyperspectral Image. The estimation problem is cast as an optimisation one in a structural optimisation setting based upon the dichromatic reflection model (Shafer, 1985).

3.4 Analysis via Establishing a Sensor Model

Given the ground truth data for the entire kill set, the relationships between objective measurements, a feature vector representation of curvature over the carcass hindquarter, and LMY were evaluated using the supervised learning for regression pipeline exploiting Gaussian Processes (Rasmussen and Williams, 2006) reported in B.SBP.0121.

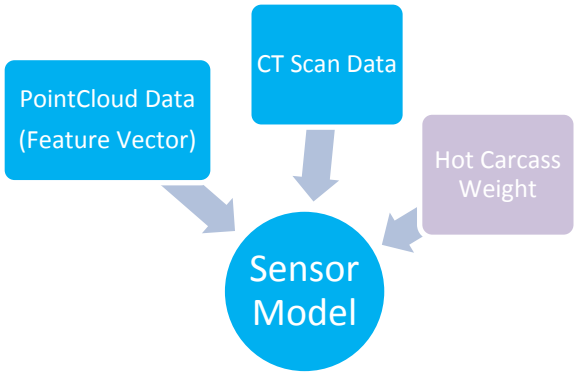

Fig. 11 - Building a sensor model from features of 3D data, CT Scan Data and Hot Carcass Weight

The approach consists of constructing a sensor model, shown in Fig. 11, to learn to characterise the feature vector (Witten et al., 2011), an accumulation of inputs (such as 3D point cloud data, i.e., feature vector), and optionally Hot Carcass Weight (HCW) [kg]). Once built, the sensor model can be used to produce the appropriate estimation of a trait (such as LMY) via regression on the presentation of an instance vector gathered from a new carcass.

To evaluate the sensor model, regression experiments were performed using 10 Cross Fold Validation on feature vectors containing a single instance of each carcass. In addition, classification experiments were repeated another 50 times, effectively providing a 50x10 Cross Fold Validation randomised learning scheme. Thus, providing an unbiased training and testing arrangement.

For estimation of fat depth using Hyperspectral data, the sensor model framework is also incorporated into the approach. However, given the process also involves pixel classification into fat and non-fat regions the coupling of a classifier and Gaussian Process regression is used as per Fig. 12. The training/testing phases in building model and evaluation predictions is used as previously described.

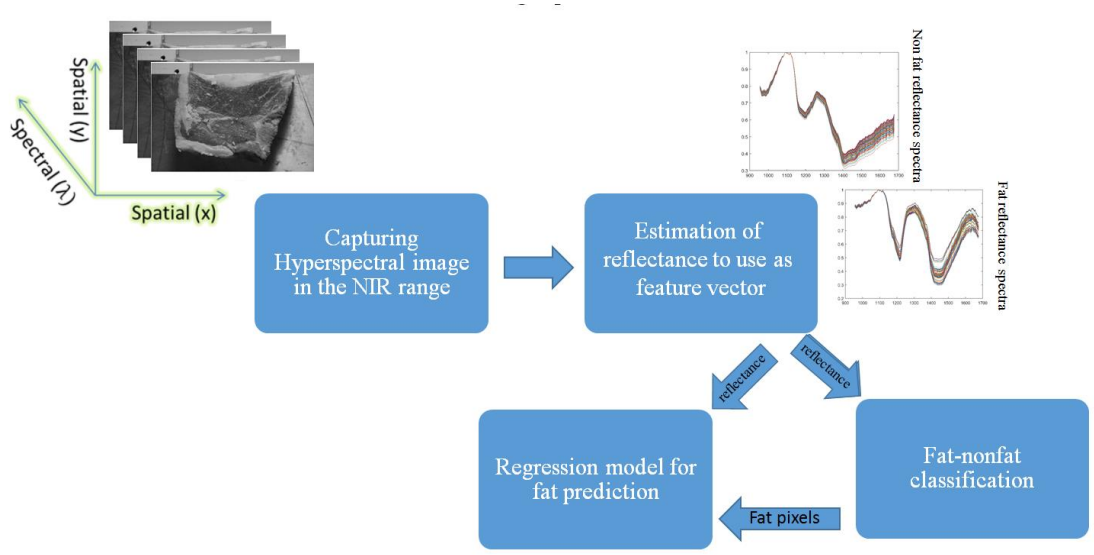

Fig. 12 - The framework for classifying muscle/fat and estimating fat depth

4 Results

4.1 Estimation of LMY in Beef Carcasses via 3D Curvatures

The technique used on beef carcasses, exploiting curvatures in hindquarter region, could be used to predict LMY. From 3D volumes, surface normals and thereafter curvatures of the hindquarter regions were extracted. Shown in Fig. 13 are surface normals over the hindquarters of the beef carcass. The pronounced changes in curvature on the left side of the beef carcass (inner side) were used as features for predicting total lean mass.

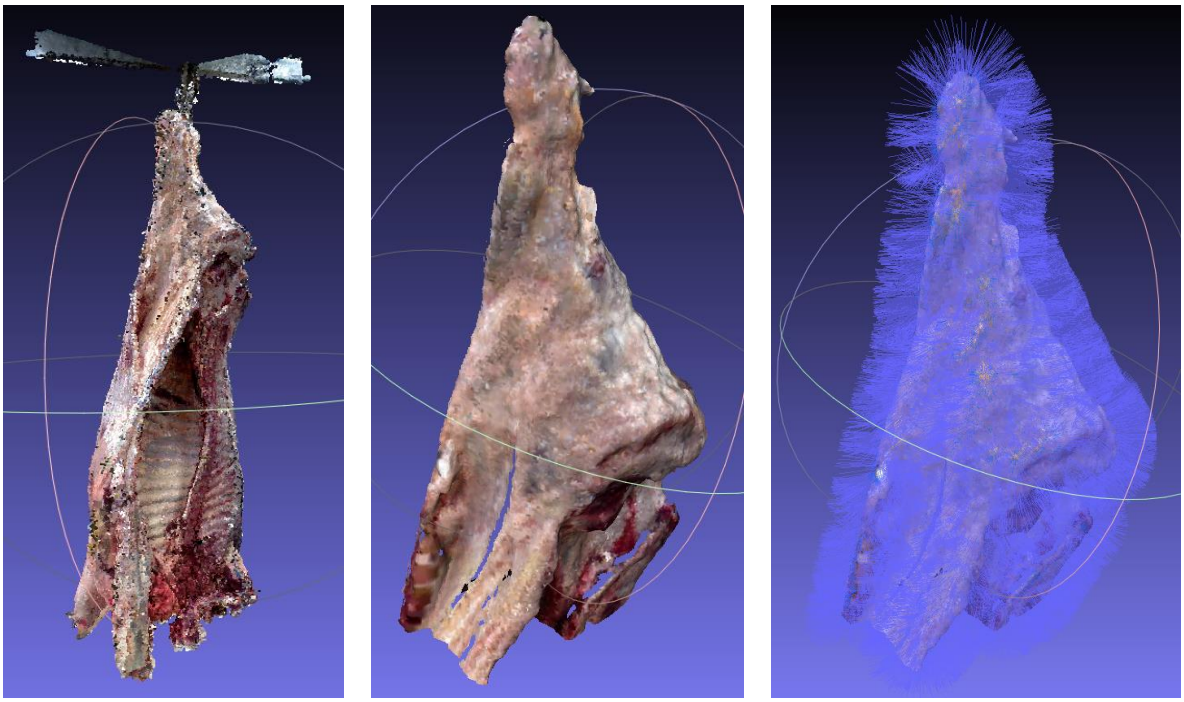

Fig. 13 - Extraction of curvatures on Beef Carcass; (left) entier carcass ; (centre) hindquarter region ; (right) surface normals extracted

The curvature of the hindquarter produced a strong relationship between lean mean yield [%] on the combined dataset, with 4.05 RMSE in estimating lean meat yield in the (n=69) carcasses. The graph comparing the measured vs estimated Lean % is presented in Fig. 14. Blue squares on the graph are associated with data from May 2016 Kill, green squares belong to May 2014 Kill and red squares the October 2016 kill. The apparent division in LMY for the two datasets is in part a result of the difference in days on feed (134 and 94 respectively), which has resulted in a larger fat deposit relative to total carcass weight, and reduced Lean % for the May 2016 kill.

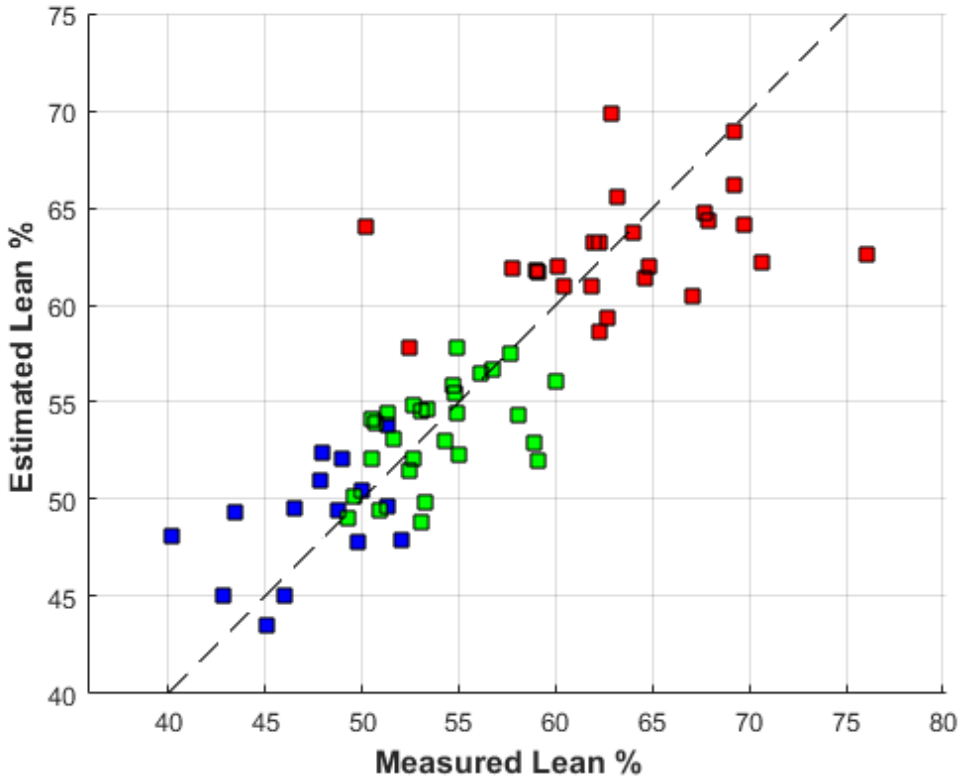

Fig. 14 – Results of the Lean % Estimation Using Curvatures, data in green is from Kill 4 at John Dee Warwick, blue Kill at TEYS Wagga and red Kill at JBS Bordertown

R^2 (coefficient of determination)	**0.7**
Mean absolute error	**3.01**
Root mean squared error	**4.05**
Range	**40.2 – 76.1 %**

4.2 Estimation of LMY in Lamb Carcasses via 3D Curvatures

After analysis of a wider number of lamb carcasses, it was evident pronounced changes in curvature were not pronounced on lamb carcass, rendering the method that solely relies on 3D curvature unable to estimate LMY (further discussion in Sect 5.2**Error! Reference source not found.**).

Instead, traits such as bone weight and fat weight were hypothesised as objective measurements to determine if these measurements would improve LMY when combined with other objective measurements. This would allow ascertaining whether it is worth developing proxies for bone weight

and fat weight in combination will allow to estimate LMY more accurately. Given metric values of all the measurements, the estimation of LMY in kg rather than LMY % was performed.

Using the subset of complete 3D models (n=33), features such as forearm length, total carcass length, volume and surface areas were derived. These features were also used in combination with easily accessible objective measurements (Hot Carcass Weight) to predict traits.

Evaluation of a number of different combinations of objective and derived measurements are in Table 3 and Table 4. The lowest error for LMY estimation was achieved using Hot Carcass Weight (HCW) alone as input Normalised Root Mean Square Deviation (NRMSD) 5.02% and 4.47% over the hindquarter and full carcass respectively. Adding input such as volume (with or without abdominal cavity removed) and EMA marginally increased the error, with EMA resulting in a larger error than volume. An example of the learning framework for these inputs is shown in Fig. 15; the source of the error in using volume to estimation lean can be seen in the rightmost graph, where carcasses with similar LMY have vastly different volumes.

Table 3 - Estimation applied to data of Carcass Hindquarters acquired in all serial slaughter #6 (N =96)

Estimate	Inputs	RMSE	MAX ERROR	RANGE	NRMSD (%)
Bone [kg]	HCW	0.22	0.62	2.6217 - 5.3032	8.3
Lean [kg]	HCW	0.75	2.17	7.9828 - 20.3051	5.69
Lean [kg]	HCW+EMA	0.70	1.75	7.9828 - 20.3051	5.30

Table 4 - Estimation applied on Full Carcasses acquired in all serial slaughter #6 (n =33)

Estimate	Inputs	RMSE	MAX ERROR	RANGE	NRMSD (%)
Bone [kg]	HCW	0.23	0.49	2.62 - 5.28	8.66
Bone [kg]	HCW + Forearm	0.24	0.57	2.62 - 5.28	9.19
Bone [kg]	HCW + Length	0.26	0.59	2.62 - 5.28	10.1
Lean [kg]	HCW	0.55	1.28	7.9828 - 20.3051	4.47
Lean [kg]	HCW+EMA	0.57	1.46	7.9828 - 20.3051	4.66
Lean [kg]	HCW + Volume*	0.57	1.32	7.9828 - 20.3051	4.86

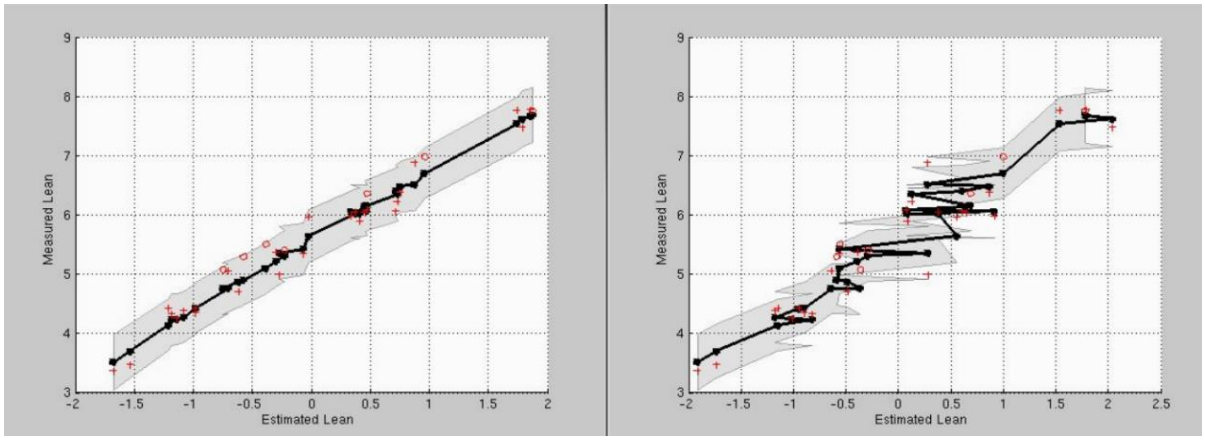

Fig. 15 - One of the folds (cross validation has 50 folds with randomly partitioned data) from the estimation process for LMY [kg] on Kill #6 Hindquarter data using as inputs: CCW (left), Volume (right). In black is the relationship between the measured and the predicted lean for each input respectively. The grey area shows the two-sigma bounds. The red circles are the data points used to build the prediction model, and the red crosses are the data points used to query the model and obtain an estimate

A number of lengths were derived from the 3D data (Forearm length and Total Length: measured from neck to tail) and used as inputs in combination with HCW to predict bone weight. The lowest error for bone weight estimation was found using HCW alone (approximately 8.5% for both hindquarter and full carcass). To determine whether proxy measurements for bone weight and fat weight could yield improved predictions for LMY, the ground truth of these measurements were hypothesised as objective measurements and used as inputs. These hypothesised rows are displayed in orange in Table 8. A significant improvement in LMY, an NRMSD of 1.36%, can be achieved if a sufficiently accurate proxy for fat can be determined.

In order to validate the predictive accuracy of the objective measurements, the experiments were repeated over all of the 2015 data (n=569), shown in Table 5 and Table 6. The hypothesis based on the Kill #6 subset was that HCW resulted in the most accurate prediction of LMY. Instead, the best predictor of LMY was a combination of HCW and EMA (4.10% NRMSD). The best predictor of Fat weight was a combination of HCW and GR (4.53% NRMSD).

The hypothesised objective measurement of fat was confirmed to be a covariate of LMY over the entire 2015 data as over the Kill #6 subset (1.40% NRMSD).

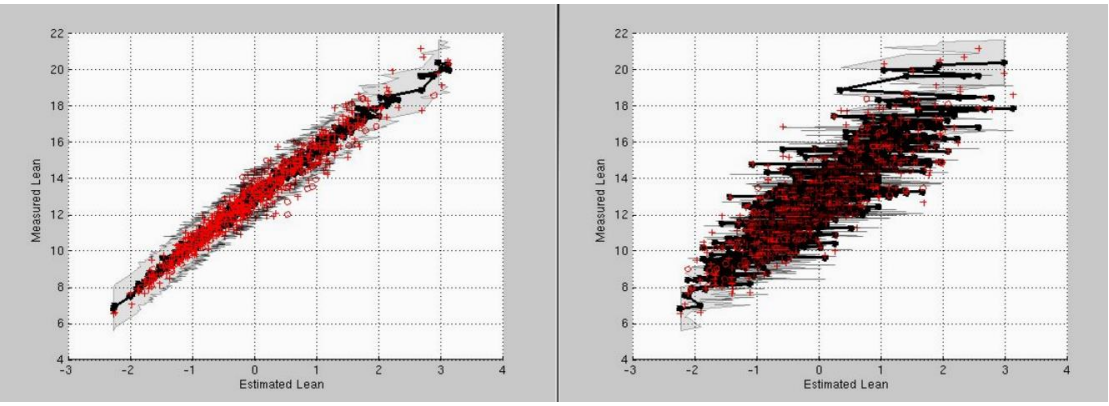

Fig. 16 - One of the folds (cross validation has 50 folds with randomly partitioned data) from the estimation process for LMY on all 2015 data using as inputs: CCW (left), EMA (right). In black is the relationship between the measured and the predicted lean for each input respectively. The grey area shows the two-sigma bounds. The red circles are the data points used to build the prediction model, and the red crosses are the data points used to query the model and obtain an estimate.

Whilst HCW and Volume marginally out-performed a combination of HCW and EMA on the Kill #6 subset, the combination of HCW and EMA performed best over the larger dataset. A consistent estimation of volume in combination with HCW could out-perform the combination of HCW and EMA, over the larger data set.

Table 5 - Estimation applied to data of Full Carcasses acquired in all serial slaughters (N =569)

Estimate	Inputs	RMSE	MAX ERROR	RANGE	NRMSD (%)
Bone [kg]	HCW	0.23	0.72	1.7988 - 5.3032	6.54
Lean [kg]	HCW	0.64	2.33	6.5391- 21.1410	4.38
Lean [kg]	HCW+EMA	0.59	2.01	6.5391- 21.1410	4.07
Lean [kg]	Weight**	0.20	0.62	6.5391- 21.1410	1.40
Fat [kg]	HCW	0.75	2.76	1.8218- 14.5705	5.88
Fat [kg]	HCW + GR	0.59	2.19	1.8218- 14.5705	4.53
CCW [kg]	HCW	0.28	3.47	10.6270- 9.5450	0.97

Weight ** = CCW – Fat Weight [kg]

Table 6 - Estimation applied to data of Carcass Hindquarters acquired in all serial slaughters (N =569)

Estimate	Inputs	RMSE	MAX ERROR	RANGE	NRMSD (%)
Lean [kg]	HCW	0.29	1.04	2.5619 - 8.2131	5.1839
Lean [kg]	HCW+EMA	0.27	0.96	2.5619 - 8.2131	4.8817

Table 7 - Estimation applied to data of Full Carcasses acquired in all serial slaughter #6 (N =96)

Estimate	Inputs	RMSE	MAX ERROR	RANGE	NRMSD (%)
Lean [kg]	HCW	0.75	2.17	7.9828 - 20.3051	5.69
Lean [kg]	HCW+EMA	0.70	1.75	7.9828 - 20.3051	5.30

Table 8 - Estimation applied on Carcass Hindquarters acquired in all serial slaughter #6 (n =33)

Estimate	Inputs	RMSE	MAX ERROR	RANGE	NRMSD (%)
Bone [kg]	HCW	0.07	0.17	0.8873 - 1.7859	8.49
Bone [kg]	Total Length	0.12	0.43	0.8876-1.7859	14.18
Bone [kg]	Volume* x Total Length	0.28	0.68	0.8876-1.7859	10.74
Lean [kg]	HCW	0.22	0.41	3.3699 - 7.7774	5.02
Lean[kg]	HCW + Volume*	0.23	0.45	3.3699 - 7.7774	5.25
Lean [kg]	HCW + Volume	0.23	0.50	3.3699 - 7.7774	5.28
Lean [kg]	HCW + EMA	0.24	0.47	3.1701 - 7.7774	5.64
Lean [kg]	Weight	0.17	0.31	3.1701 - 7.7774	3.91
Lean [kg]	Weight*	0.19	0.34	3.3699 - 7.7774	4.31
Lean [kg]	Weight* + Volume	0.19	0.42	3.3699 - 7.7774	4.44
Lean [kg]	Weight^{+}	0.05	0.12	3.3699 - 7.7774	1.35
Lean [kg]	Weight^{+} + Volume	0.06	0.12	3.3699 - 7.7774	1.45
Weight [kg]	Volume	0.59	1.37	4.9370- 12.3260	8.10
Weight [kg]	HCW	0.21	0.43	4.9370- 12.3260	2.92

Weight specifically refers to the Total Weight of Hindquarter (provided)
Weight* = Total Hindquarter Weight – Bone Hindquarter Weight [kg]
Weight + = Total Hindquarter Weight – Fat Hindquarter Weight [kg]
Weight specifically refers to the Total Weight of Hindquarter (provided)
Volume* = Indicates hindquarter acquired volume from 3D data with removal of abdominal cavity

4.3 Estimation of Fat Depth in Lamb via Hyperspectral Camera

A total of 14 specimens were analysed. As the Hyperspectral Camera approaches based on radiance traditionally rely on complete illumination control the light source was moved to two positions during each data acquisition, to evaluate the robustness of the approach. The fat depth estimation results presented in Fig. 17 on the limited dataset have a RMSE of 0.8mm with full curves noted Fig. 18.

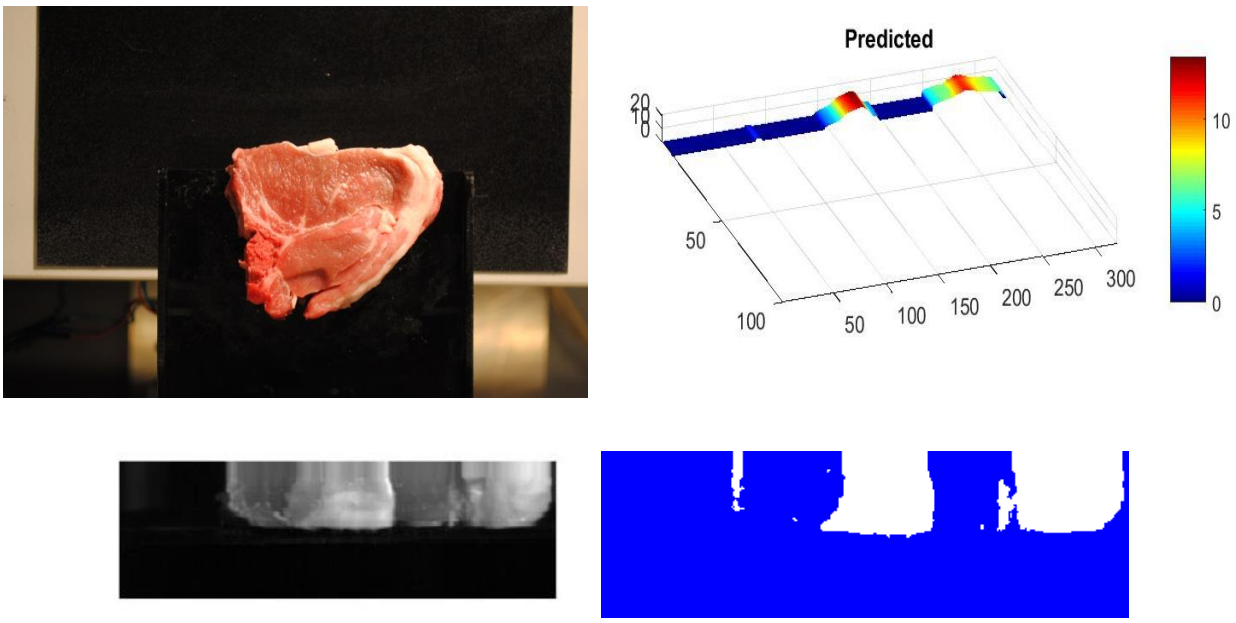

Fig. 17 – Fat depth Estimation, anti-clockwise from top left: (1) top down view of cut of lamb, (2) Hyperspectral data obtained when looking at the cut from the side, (3) the produced separation of muscling and fat of the side view, (4) reconstructed fat profile from side view, this correlates to fat visible in top down view.

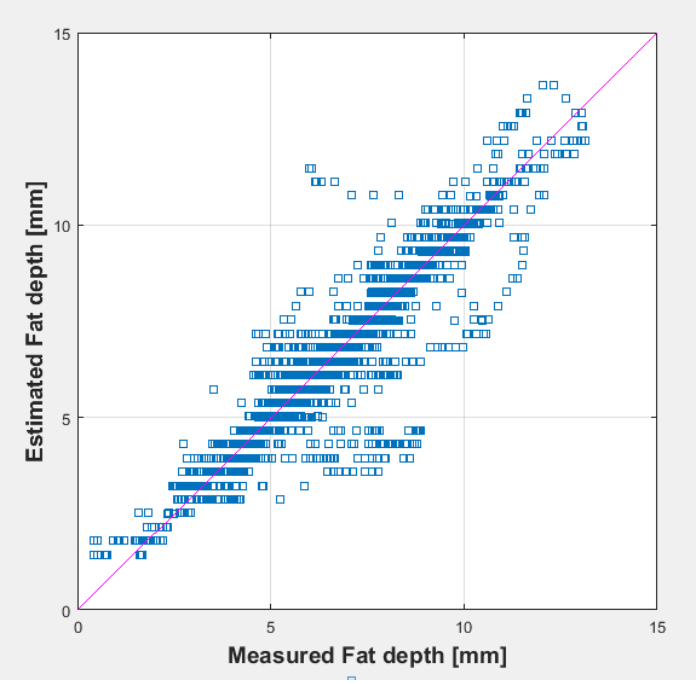

Fig. 18 –Estimated vs Actual fat depth

Table 9 –Statistics of estimating fat depth [mm] (using Reflectance)

R^2 (coefficient of determination)	**0.92**
Mean absolute error	**0.69**
Root mean squared error	**0.80**
Range / Mean [mm]	**1-13 / 8.2**
Dataset size (pixels)	**3069**

5 Discussion

5.1 Estimation of LMY in Beef Carcasses via 3D Curvatures

The work reported contained an approach to 3D carcass construction that exploited the frames of data from multiple RGBD cameras contained on the scanning rig simultaneously via a batch optimisation framework (g2o) to compute the best fit of all data into a common representation of the carcass. This improved pipeline has resulted in denser 3D information, more coverage over the carcass and increased robustness to sensor noise. This work has further allowed an evaluation of possibilities for speeding up the up the acquisition process of the 3D scanner.

Over the period May 2016 – October 2016 two field trials were conducted with the 3D scanner; with an overall 14-day deployment in non-spray chillers at TEYS Wagga Wagga and JBS Brooklyn. A total of 71 beef carcass sides were scanned by the system. Several avenues for improving the current design in mechatronics aspects were actioned such as mechanisms for actuating (controlling the cameras), cable management and the modularity of component assembly for ease of transportation and installation. The new design was tested in chillers at UNE though the long planned test in John Dee (March 2017) was aborted due to lack of space for the scanner (oversupply in chillers at John Dee).

The data acquisition process of beef carcasses also determined that the system needed a larger footprint (increase radius by 20cm) to deal with the beef carcasses that exceeded the allocated carcass space available within the scanner and were subsequently too close to the RGBD cameras for 3D information to be captured. An alternative camera system with shorter range (Intel Realsense SR300) is being investigated as well as methods exploiting RGB only data to extract missing 3D information.

Data from field trial on beef carcasses (TEYS Wagga Wagga, May 2016) were combined with data acquired in the preceding project (John Dee Warwick, May 2014), allowing testing the extendibility and portability of utilising 3D curvatures for estimating LMY. The curvature of the inner surfaces of hindquarters produced a strong relationship on the combined dataset with 4.05 RMSE in estimating LMY. There appear to be marginally larger errors on some carcasses within the boundaries of the two datasets which will be further investigated, with the difference in sampling resolution a possible cause.

An indicator of the importance of muscle delineation was previously identified in preliminary attempts to partition the lamb carcass along muscle groups, where removing the abdominal void yielded an improvement in LMY estimation accuracy when compared to using the entirety of the hindquarter volume. The muscle group extraction is also to a less pronounced extent affecting the LMY in beef carcasses. The hindquarter boundary is still being semi-autonomously extracted and significantly more focus will be emphasised on improving the consistency and accuracy of muscle grouping.

5.2 Estimation of Fat Depth in Lamb via Hyperspectral Camera

The capacity of Hyperspectral Imaging to determine the depth of fat present at the surface of the lamb carcass is being developed and tested in order to assist in estimating carcass fat and therefore LMY. Traditional Hyperspectral Imaging approaches use radiance from the data, which is only viable from surfaces which are perpendicular to the view direction of the camera. In the scenario we are proposing, the Hyperspectral Camera will be affixed to the existing scanning rig alongside the RGBD cameras. Since RGBD cameras provide information about the carcass surface normals, and the position of the Hyperspectral Camera is known relative to the depth cameras, it will be possible to combine the Hyperspectral Imaging data with 3D data to leverage both technologies in a novel way.

At present, preliminary studies in a laboratory setup on cuts of lamb have reaffirmed the capability of Hyperspectral Imaging to produce a delineation of muscling and fat at significantly high accuracy, above 98%. Reflectance, which is estimated from the photometric and geometric properties of data in hundreds of bands across the NIR spectrum, is used to estimate fat depth of data. A RMSE of 0.9 was achieved in estimating fat depth, with current evaluations indicating the capability to discern fat depth is limited to 12mm, significantly more than previously anticipated. This capability will potentially allow for fat cover estimation. It is anticipated that subcutaneous fat cover and overall fat are strongly related (given lamb have little inter-muscular fat) thereby estimating a proxy for GR8 or total fat and thereafter total lean of a carcass is viable.

5.3 3D Carcass Generation Anomalies

5.3.1 Rig design limitations

Ongoing development of the rig in response to challenges encountered has caused some data losses in part production environments, due to the time-sensitive nature of the abattoir. The updated rig prevents cable entanglements with cable chains, cable guards, and an updated more streamlined and powerful camera platform and pulley system, as shown in Fig. 19. A base redesign specific to Beef Carcases is being undertaken to cater for the increased breadth of the carcasses encountered.

Fig. 19 - Scanning rig redesign employed in Lamb Carcass 3D and Hyperspectral data collection

5.3.2 RGBD sensing range limitations

The Primesense Carmine 1.09 cameras used (proprietary component of Apple Inc) have a minimum range of 0.3 meters. The rig has a radius of approximately 0.7 meters. When scanning the larger carcasses, it is possible for parts of the carcass to be too close to the camera, and depth data is not available. An example of the missing region of the carcass is shown in Fig. 20. The fusion pipeline can recover from the loss of some depth data, but when the missing region is too large, or if it involves some of the region of interest, then fusion results are compromised.

The solution to this problem is two-fold. The first is to prevent the loss of depth data, either through redesigning the rig to prevent the camera from ever being too close to the carcass, or in changing camera models to one with a smaller minimum range. New camera options, such as the Intel Realsense SR300 (https://software.intel.com/en-us/realsense/sr300camera) are being investigated as they have a 0.1m minimum sensing region and higher quality RGB images to assist fusion. The second solution is to leverage, in the fusion software pipeline, the RGB data alone to cover regions where depth data is not available. This approach is currently being investigated.

Fig. 20 - Parts of carcass within minimum sensing rage of Primesense Carmine 1.09 RGBD sensor (30cm minimum sensing range)

5.3.3 Fusion pipeline problem cases

As part of the data collection at JBS, several cows were scanned. Due to the thinness of the carcass relative to the sensor noise, a correct Poisson surface could not be fitted to the pointcloud. Rather than correctly fit a surface to the outer and inner surfaces of the cow, the Poisson algorithm fitted a single surface through the set of points, as shown in Fig. 21.

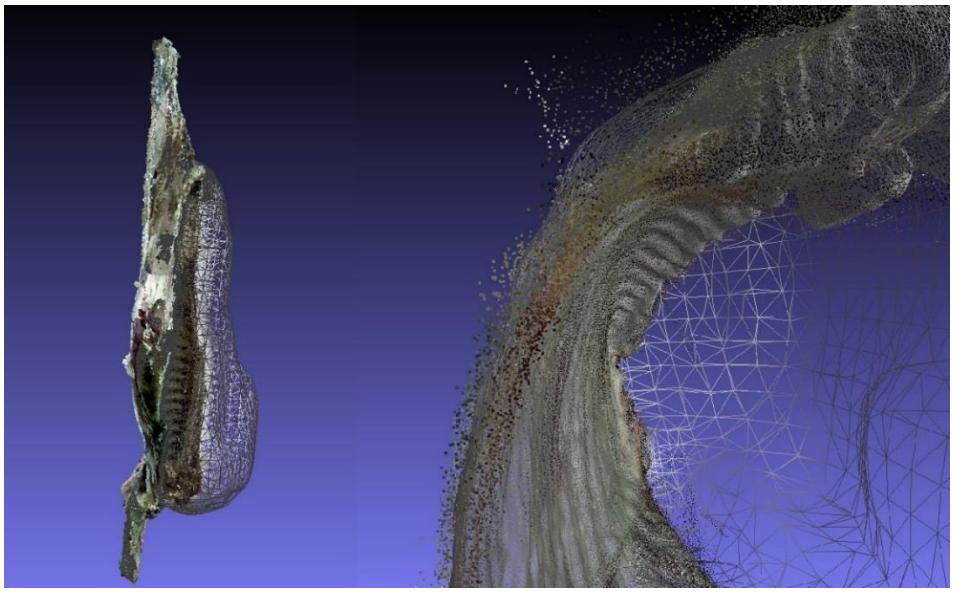

Fig. 21 - Poisson surface incorrectly fitted to the cow carcass. The left shows the entire carcass. The right shows a larger view looking down through the cow's ribcage, showing that a surface has been fitted through the middle of the points.

This problem has motivated further work into reducing and managing sensor noise. Alternative approaches to replace Poisson surface-fitting could also be investigated.

Poisson surface fitting depends on the quality of the surface normals generated from the pointcloud. For most carcasses, a radius of 10 nearest neighbours was sufficient to generate accurate normals and fit a Poisson surface. For other carcasses, a radius of 10 nearest neighbours was not sufficient and resulted in inconsistent surface normals as seen Fig. 22. Inconsistent normal manifested in particular around deeply recessed surfaces of the carcass. The resulting Poisson surfaces were liable to be missing regions of the carcass, with high errors around the aforementioned deeply recessed surfaces.

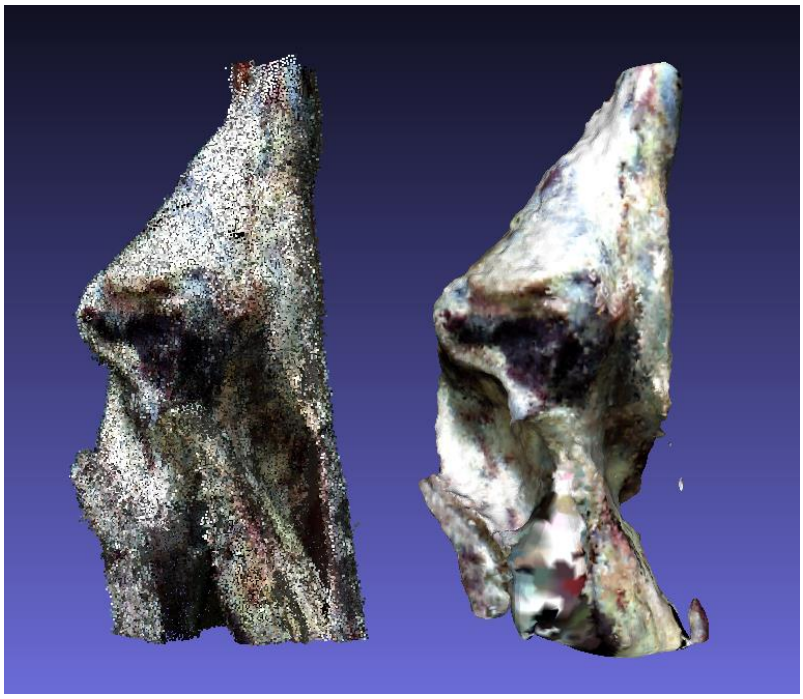

Fig. 22 - Left: the pointcloud of a carcass hindquarter. Speckled dark and light points show the inconsistent surface normals. Right: the Poisson surface, with missing regions.

A solution to this problem was to change the parameters used to generate surface normals. The cost of this is a smoother mesh, which might potentially lose surface curvature features required as part of the LMY estimation. Solving the previous problem addressing sensor noise will also alleviate this problem with surface normal generation.

5.4 Mapping to Project Objectives

Finally, a reflection on the status of the project with respect to project objectives is undertaken.

1. ***Determine the best camera position for estimating Lean Meat Yield in lamb carcasses***

While obtaining 3D imaging data of lamb carcasses was demonstrated as practical and achievable within operational constraints of abattoirs, the 3D curvatures did not related to LMY. Therefore, the process of estimating subcutaneous fat with Hyperspectral imaging was proposed, leveraging 3D curvatures in this process. Obtaining calibrated Hyperspectral to CT scan data to establish and quantify this relationship has not yet been established, and is unique to the approach presented. A field trial at UNE (UNE Chillers) and Armidale Radiology was undertaken in March 2017 with preliminary investigation having taken place indicating the fundamental science behind this approach is being established and our 3D approached to data fusion could be leveraged for this task.

2. Develop and validate the machine learning of 3D images of lamb carcasses to estimate lean meat yield

Advances have been made to further quantify the relationship, the current results indicate the surface shape of hindquarter shows potential to map to LMY via Volume with the assistance of hot carcass weight. However, the process of extracting the region for curvature estimation needs more precise estimation of muscle delineation, as inconsistency in this aspect alone can lead to increased error.

3. Benchmark prediction accuracy in commercial processing conditions against CT (lamb) and CT or commercial bone out (beef)

The curvature of the hindquarter produced a strong relationship between lean mean yield [%] on beef carcasses on a combined dataset of (n=69, three kills), with 4.05 RMSE and 0.7 R^2. The use of 3D curvature did not generalise to lamb carcasses.

4. Deliver prototype devices to estimate traits of carcass

Over the period September 2015 – October 2016, three field trials were conducted with the 3D scanner; with an overall 15-day deployment in non-spray chillers at JBS Brooklyn, TEYS Wagga Wagga and JBS Brooklyn, attesting durability in harsh settings. Several avenues for improving the current design in mechatronics aspects were actioned such as mechanisms for actuating (controlling the cameras), cable management and the modularity of component assembly for ease of transportation and installation. The new design was tested in chillers at UNE though the long planned test in John Dee (March 2017) was aborted due to lack of space for the scanner (oversupply in chillers at John Dee).

6 Conclusions/recommendations

The fusing of 3D data from the depth cameras has shown a capability to capture 3D geometry, and underlying shape differences. The quality of the predictions are dependent on several aspects (1) the accuracy of the 3D representation (2) consistency of muscle group extraction and (3) the amount of data provided for training.

The 3D fusion framework can be further automated and improved by incorporating initial estimates of camera locations and directions from the motors. Varying speeds of camera travel actively in response to motion of the carcass to avoid zones where information from depth sensors is not possible (proximity to camera). In cases where depth data is not available, using RGB data alone to generate 3D pointclouds is warranted. More robust loop closure (i.e. finding matches between camera sequences) is needed. While some of these problems will be dealt with by the newly implemented hardware improvements, improvements are also being made to the software so that anomalies in data collection can be handled gracefully and still result in successful mesh fusion.

Currently the mesh generated by the fusion pipeline is semi-autonomous, the region of interest for lean meat yield estimation is extracted by gross carcass height ratios. Methods to extract muscle groups from the 3D model (via seams of muscles visible on the exterior and interior of carcass) should be investigated. The approach of modelling the non-rigidly deforming scenes as presented by Newcombe (2015) will be evaluated in extracting the muscle groups. Using the surface normal

information to find boundaries between regions of the carcass will help in automating this mesh cutting step, such as Fig. 23, as well as making results more objective and consistent across carcasses.

As with any data driven machine learning approach, the breadth of data allows the machine learning framework (i.e. Gaussian Processes used in this work) to establish a mapping between the features (high dimensional space of 3D curvatures) and the estimated measure (LMY). Given only surface attributes are being examined, current work indicates that additional features related to Carcass Weight, gender or allometric growth could possibly yield a hierarchical / stratified learning scheme rather than a one-for-all modelling approach.

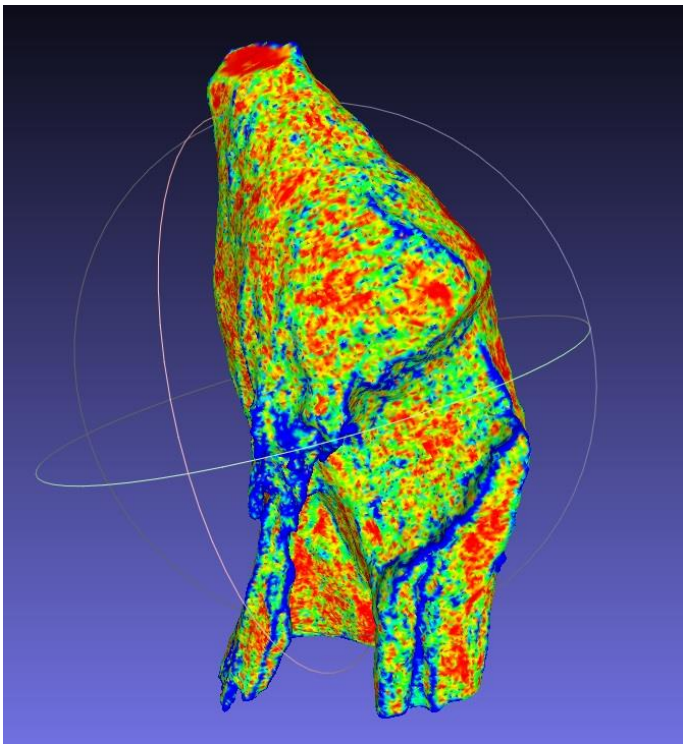

Fig. 23 - Exploiting surface normals to identify regions of the carcass

Finally, using Hyperspectral, data alone has potential to provide a more accurate fat cover estimation. However, challenges of light source direction relative to surface examined are present, and not easily circumvented with a sole sensor. Leveraging 3D information to compliment the Hyperspectral sensor data has the potential to substantially improve and increase underlying robustness of fat cover estimation. This combination of data is novel and could either compliment GR8 fat depth measurement or provide a proxy for total fat cover or total fat, thereby LMY.

7 Bibliography

Huynh, C. P., & Robles-Kelly, A. (2010). A solution of the dichromatic model for multispectral photometric invariance. International Journal of Computer Vision, 90(1), 1-27.

Kümmerle, R., Grisetti, G., Strasdat, H., Konolige, K., & Burgard, W. (2011, May). g 2 o: A general framework for graph optimization. In Robotics and Automation (ICRA), 2011 IEEE International Conference on (pp. 3607-3613). IEEE.

Newcombe, R. A., Fox, D., & Seitz, S. M. (2015). Dynamicfusion: Reconstruction and tracking of non-rigid scenes in real-time. In Proceedings of the IEEE conference on computer vision and pattern recognition (pp. 343-352).

Shafer, S. A. (1985). Using color to separate reflection components. Color Research & Application, 10(4), 210-218.

Rahman, S., & Robles-Kelly, A. (2013). An optimisation approach to the recovery of reflection parameters from a single hyperspectral image. Computer Vision and Image Understanding, 117(12), 1672-1688.

Rasmussen CE, Williams C, K. I. . Gaussian Processes for Machine Learning (Adaptive Computation and Machine Learning): The MIT Press; 2005.

Witten I, Frank E, Hall M (2011) Data Mining – Practical Machine Learning Tools and Techniques, Ed 3

Zanuttigh, P., Marin, G., Dal Mutto, C., Dominio, F., Minto, L., & Cortelazzo, G. M. (2016). Time-of-flight and structured light depth cameras. Heidelberg: Springer.

8 Appendix

8.1 Acknowledgments

Team from UTS: Alen Alempijevic, Phillip Quin, Sejuti Rahman, Teresa Vidal Calleja, Tristan Walsh

Team from NSW DPI: Malcolm McPhee, Edwina Toohey

Team from Murdoch: Graham Gardner

We extend our thanks to JBS staff (Graham Treffone, Mark Kelly, Darrel Cody), Murdoch Team (Graham Gardner, Jarno, Chris Smith, C.J), Scott Automation Team (Jonathan Cook, Victor Martchenko, Paul Danelutti), NSW DPI (Malcolm McPhee, Dan Ebert), and for the data obtained at serial slaughters conduct at JBS Bordertown.

We express gratitude to staff at TEYS Wagga Wagga (Grant Garey, Jasmine Nixon) NSWDPI staff (Malcolm McPhee, Reg Woodgate, Edwina Toohey, Jason Siddell) that assisted our team in obtaining beef carcass data reported.